Dynamics of Poly(cyclohexyl methacrylate): Neat and in Blends with Poly(α-methylstyrene)

C. M. Roland*,† and R. Casalini‡

Naval Research Laboratory, Chemistry Division, Code 6120, Washington, DC 20375-5342, and Chemistry Department, George Mason University, Fairfax, Virginia 22030

ABSTRACT: Pressure−volume−temperature measurements, calorimetry, and dielectric spectroscopy at ambient and elevated pressures were carried out on poly(cyclohexyl methacrylate) (PCHMA) and its blend with poly-(α-methylstyrene) (PaMS). Both the glass transition temperature and local segmental relaxation times, τ_α, go through a maximum as a function of blend composition, plausibly due to a negative excess volume. Using a nonlinear function for the composition dependence of T_g, a value of the self-concentration parameter of the Lodge−McLeish model is determined, which is close to that calculated from the PCHMA chain statistics. For both neat PCHMA and the blend, the τ_α superpose as a function of TV^γ. Since the breadth of the local segmental relaxation dispersion is a unique function of τ_α, this means that the parameter γ defines both the magnitude and distribution of relaxation times. The thermodynamic scaling for the blend was corroborated by calculating the exponent γ from the isochronal thermal expansion coefficient, determined from the pressure coefficient of T_g. γ increases upon blending, consistent with a larger activation volume of PCHMA when mixed with the PaMS. PCHMA exhibits a weak β-relaxation, which lacks correspondence to the segmental dynamics and thus is presumably due to local motion of the carbonyl group. A more intense γ-relaxation and a frequency-insensitive loss at higher frequencies are also observed. Unlike the segmental process, these secondary relaxations are insensitive to blending.

1. Introduction

On approach to the glassy state, the local segmental relaxation of polymers, involving correlated conformational transitions of a couple of backbone bonds, undergoes dramatic changes in rate (by many orders of magnitude) over a small range of temperatures, *T*. This change in local segmental relaxation time, τ_α, is accompanied by large changes in physical properties as well as the appearance of diverse phenomena such as the dynamic crossover,[1,2] decoupling of translational and reorientational motions,[3−5] and bifurcation of the local segmental dynamics to form the Johari−Goldstein secondary process.[6−8] Notwithstanding the many property changes, the conformation of the polymer chains remains essentially the same throughout the glass transition regime. This fascinating behavior is also observed in the structural relaxation of liquids, for which molecular rotation is the counterpart to the conformational backbone transitions of polymers. Although near the glass transition polymeric and molecular glass-formers cannot be distinguished by their dynamics, there are some subtle differences in properties. One of the most significant is that the dependence of τ_α on *T* for polymers is more an effect of temperature than of the accompanying volume change, whereas the volume changes per se exert a stronger influence on the dynamics of small molecules.[9,10]

When mixed with a second component, the dynamic behavior of polymers and small molecules can be quite different, with experiments on polymer blends yielding insights into the glass transition not otherwise available. This is because a characteristic of polymer blends is concentration fluctuations, which broaden the glass transition[11−13] but are less important for small molecule mixtures due to the latter's large combinatorial entropy. The chain character of polymers also causes deviations in local composition away from the mean.[14−17] These effects, concentra-

tion fluctuations and chain connectivity, give rise to dynamic heterogeneity, as first seen in NMR measurements on blends of polyisoprene and polyvinylethylene.[18] In a dynamic heterogeneous blend each component exhibits distinct relaxation properties, whereby two relaxation dispersions are apparent in the spectrum. Measurement of the component dynamics allows the influence of inherent mobilities (related to structural bulkiness, chain flexibility, etc.) to be distinguished from effects due to the local environment (e.g., intermolecular interactions and constraints). The severity of intermolecular constraints can be varied by changing the relative rate of the component dynamics, for example by changing their T_g. This can be accomplished by variation of their molecular weights, which does not involve any changes in chemical structure.

Various models for the component dynamics in polymer blends have been proposed[19−27] and were recently reviewed.[28] A popular approach is due to Lodge and McLeish (LM),[25] who addressed the effect of local composition on the segmental dynamics in blends with a model based on the idea that the relaxation rate of a segment in a blend is determined by the composition of its local volume, and the size of the latter is governed by the chain flexibility. The LM model offers the possibility of predicting the blend dynamics solely from the properties of the neat components.

In this work we describe dielectric relaxation measurements at ambient and elevated hydrostatic pressure on poly(cyclohexyl methacrylate) (PCHMA), both neat and blended with poly(α-methylstyrene) (PaMS). PCHMA and PaMS form thermodynamically miscible blends, with their lower critical solution temperature exceeding 560 K (approaching decomposition temperatures), even for high molecular weight components.[29] Previously, several groups have carried out ambient pressure dielectric measurements on high molecular weight PCHMA.[30−33] Herein we study a lower molecular weight sample in order to obtain a relatively low T_g. This facilitates dielectric measurements under pressure but also enables an interesting anomaly

† Naval Research Laboratory.
‡ George Mason University.

to be observed—the blend dynamics are not intermediate to the pure component dynamics. In an earlier work,[34] we found that for both neat PCHMA and its blend with PaMS the α-dispersion (or local segmental relaxation peak) is invariant to T and P for constant value of τ_α. Herein we show that the segmental relaxation times for both neat PCHMA and the blend, measured for different conditions of T and P, collapse onto single, component-specific master curve when plotted vs TV^γ, where V is specific volume and γ a material constant. Since the relaxation time defines the shape of the α-dispersion, this means that the scaling exponent γ governs not only the T and V dependences of τ_α but also the breadth of the α-relaxation spectrum. In addition to the local segmental dynamics, the dielectric spectrum of PCHMA reveals a β- and γ-relaxation.[31–33] We characterize the response of these various dynamic processes to blending and compare the results to predictions from models.

2. Experimental Section

The PCHMA (from the Polymer Source) and PaMS (Polymer Standards Service) had respective weight-average molecular weights of 3.4 and 1.5 kg/mol, with polydispersities equal to 1.14 and 1.29; both were used as received. Various blend compositions were prepared by dissolution in chloroform, followed by drying in vacuo 1 week at 333 K. Only a 50 wt % mixture was studied by dielectric spectroscopy.

Dielectric measurements were carried out using a parallel plate geometry (2 cm diameter and 50 μm Teflon spacers), with the sample molded between the electrodes at ~160 °C and light pressure. Isothermal spectra were obtained using an IMASS time domain dielectric analyzer ($10^{-3}–10^3$ Hz) and a Novocontrol Alpha analyzer ($10^{-2}–10^6$ Hz). Temperature was controlled using a Cryo Industries closed-cycle helium cryostat with a helium atmosphere (±0.02 K stability). Segmental relaxation was measured only in the liquid state; for secondary relaxation measurements in the glassy state, temperature was changed at 3 K/min with a 5 h soak time. The effect of the cooling rate on the secondary relaxations was not investigated. For measurements at elevated pressure, the sample capacitor assembly was contained in a Manganin cell (Harwood Engineering), with pressure applied using an Enerpac hydraulic pump in tandem with a pressure intensifier (Harwood Engineering). Pressures were measured with a Sensotec tensometric transducer (resolution = 150 kPa). The sample assembly was contained in a Tenney Jr. temperature chamber (±0.1 K precision at the sample). Temperature calibration for the high-pressure measurements was achieved by matching $\tau_\alpha(T)$ at 0.1 MPa to values measured in the cryostat.

Volume changes as a function of pressure and temperature were determined with a Gnomix instrument,[35] utilizing mercury as the confining fluid. Samples with ~1 mL volume were molded in vacuo. At each pressure, samples were cooled from the liquid state at 0.5 K/min through T_g, with the glass transition temperature defined from the intersection of the extrapolated liquid and glassy state volumes (using quadratic and linear $V(T)$ functions, respectively). The differential data were converted to specific volumes using the value determined at ambient conditions by the buoyancy method. Differential scanning calorimetry employed both a Perkin-Elmer DSC 7 and a TA Q100, with samples cooled from the liquid state at 10 K/min through T_g, the latter defined as the midpoint of the heat capacity change. Successive DSC scans gave results reproducible to within the reported error.

3. Results

3.1. Glass Transition and Local Segmental Relaxation at Ambient Pressure.
In Figure 1 are shown the calorimetric glass transition temperatures vs composition (by weight) for the PCHMA/PaMS mixtures. T_g for PCHMA is higher than for PaMS, but the blend data go through a maximum; that is, blends having 50% or more PCHMA exhibit a higher T_g than either
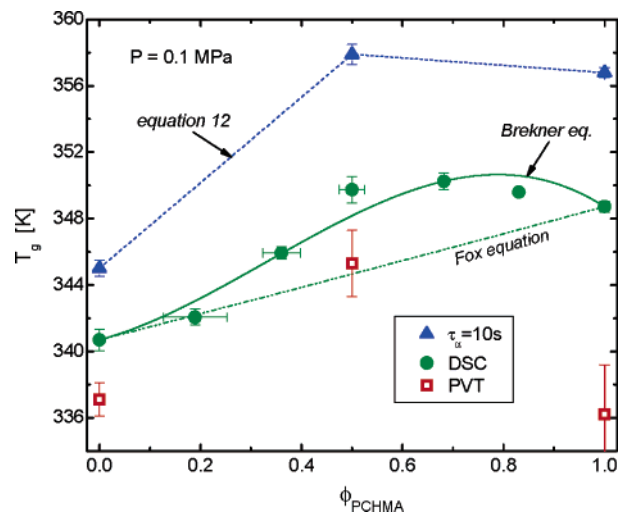

Figure 1. Calorimetric T_g vs blend composition (circles), along with the fits to eq 8 (dotted line) and eq 9 (solid line). Also shown for three samples only are the temperatures at which $V(T)$ for the liquid and glassy states intersect (squares) and the temperatures at which the local segmental relaxation time measured dielectrically equals 10 s (triangles). For the latter the $\phi = 0.5$ datum is fit to the modified LM equation yielding $\phi_{eff} = 0.60$ (dashed line).
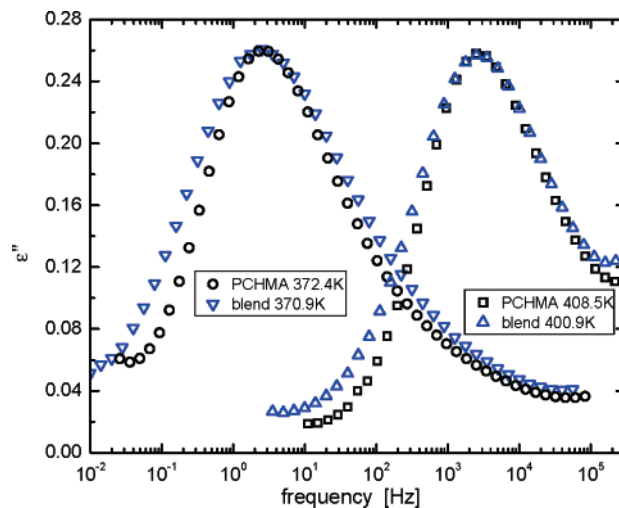

Figure 2. Representative local segmental relaxation peaks at two temperatures for the PCHMA neat and in the 50% blend with PaMS. The broadening for the latter is primarily toward the low-frequency side. (Dielectric loss values for the blend were multiplied by 2.6–2.9 to superpose the peaks.)

neat component. This same trend is seen in the ambient pressure glass transition temperatures obtained from *PVT* measurements.

Figure 2 compares the local segmental dispersion for neat PCHMA and a blend with 50% PCHMA. The dielectric response of the latter reflects motion of the PCHMA segments, since the dielectric strength for PCHMA segmental relaxation is almost a factor of 40 larger than that of the less polar PaMS. Two temperatures are shown, chosen because τ_α for neat PCHMA and the blend are equal. Thus, no horizontal shifting of the spectra was necessary, although the dielectric loss for the blend was shifted upward (by a factor of 2.90 at 370.9 K and 2.64 at 400.9 K) to match the peak values for neat PCHMA. Addition of the PaMS is seen to broaden the dispersion (otherwise, the vertical shift factor used to superpose the peak maximum for the blend would equal ~2, reflecting the 50% PCHMA concentration), and this is true for all conditions.

τ_α (defined from the frequency of the peak maximum and thus the most probable value of the local segmental relaxation
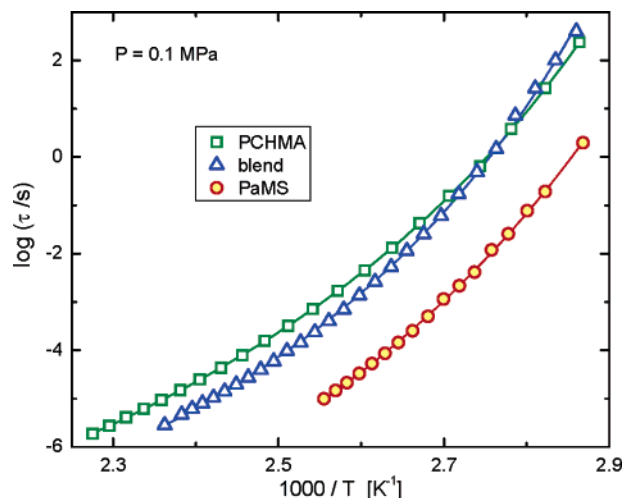
Figure 3. Local segmental relaxation times for the two neat polymers and their blend. The solid lines are the fits to eq 1 with the parameters given in Table 1. At lower temperatures τ_α is larger in the blend than for neat PCHMA.

Table 1. Local Segmental Relaxation Properties

	PCHMA	50/50 blend	PaMS
T_g(DSC) (K)[a]	348.7 ± 0.3	349.8 ± 0.8	340.7 ± 0.7
T_g(PVT)[a]	336 ± 3	345 ± 2	337 ± 1
$T(\tau_\alpha = 10\text{ s})$ (K)[a]	357 ± 0.3	358 ± 0.6	345 ± 0.5
V_g (mL/g)[a]	0.961 ± 0.001	0.958 ± 0.001	0.970 ± 0.001
$\log \tau_0$ (s)[b]	-12.31 ± 0.04	-12.26 ± 0.18	-14.8 ± 0.4
B (K)[b]	2484 ± 20	2055 ± 71	2700 ± 190
T_0 (K)[b]	275.7 ± 0.4	290.1 ± 1.4	271 ± 3
m^a	58.5 ± 0.5	70 ± 4	73 ± 5
$\beta_{KWW}(T_g)$	0.41 ± 0.01		0.30 ± 0.01
γ (eq 4)	2.5	3.7	2.7[a]

[a] $P = 0.1$ MPa. [b] Equation 1.

time) measured at atmospheric pressure for the two neat polymers and their 50/50 blend are shown in Figure 3. The data were fit to the Vogel−Fulcher equation[36]

$$\tau_\alpha(T) = \tau_0 \exp\left(\frac{B}{T - T_0}\right) \qquad (1)$$

with the best-fit values of the constants τ_0, B, and T_0 given in Table 1. At the lowest temperatures the relaxation times of the blend, due to segmental motion of the PCHMA, *are larger* than τ_α for neat PCHMA. This confirms the DSC and *PVT* results that addition of lower T_g PaMS increases the blend T_g. The temperatures at which $\tau_\alpha = 10$ s are included in Figure 1, showing the maximum vs composition.

3.2. Secondary Relaxations at Ambient Pressure. There is a weak secondary relaxation on the low-frequency side of the α-peak. It is only clearly resolved when the segmental relaxation becomes sufficiently slow, at temperatures below the glass transition. This can be seen in the spectra in Figure 4 for $T < 346$ K. The β-secondary relaxation times, τ_β (defined again from the peak frequencies), are shown in Figure 5 for PCHMA neat and in the blend at $P = 0.1$ MPa. Because of overlap with the segmental relaxation (Figure 2), τ_β can be determined only over a narrow range. Keeping in mind this limitation, there is no discernible effect of blending on τ_β. Fitting the combined data, we obtain for the activation energy $E_\beta = 90.5 \pm 2.6$ kJ/mol (Table 2) with a preexponential factor $\log(\tau_0/\text{s}) = -17.1 \pm 0.7$. This activation energy is comparable to values found for various acrylate polymers[37] but significantly higher than the $E_\beta = 73$ kJ/mol reported by Murthy and Shahin for a high molecular weight PCHMA.[33]

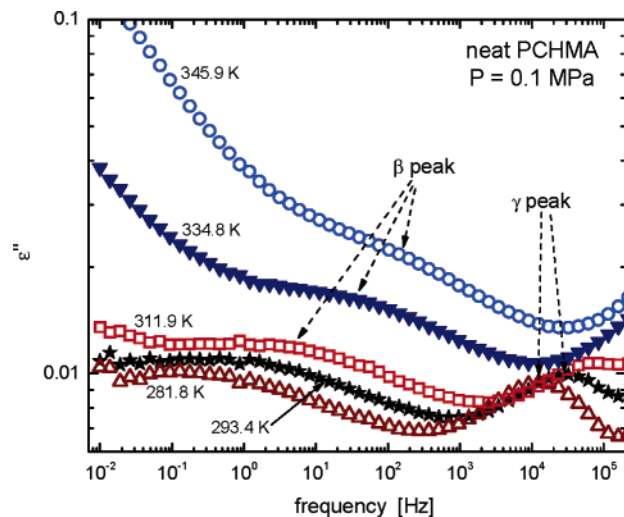**Figure 4.** Dielectric loss measured at temperatures for which the weak β-peak is evident in the spectrum. At higher temperature the strong α-process intrudes from the low-frequency side. The γ-peak can be seen at frequencies beyond $\sim10^4$ Hz.
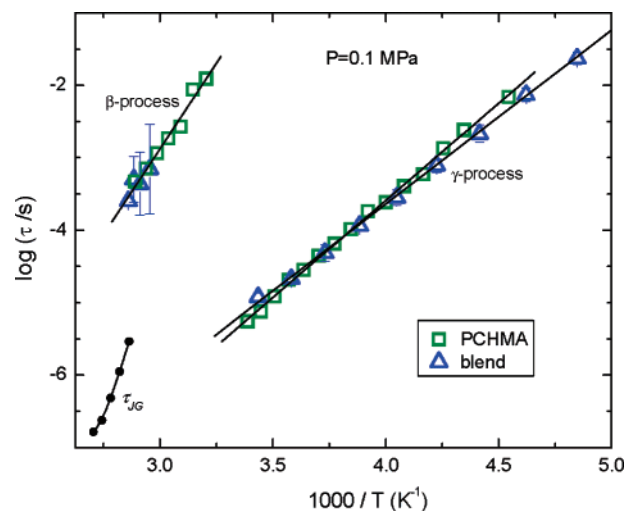

Figure 5. Relaxation times for secondary relaxations in PCHMA neat and in a 50% blend with PaMS. The lines are fits yielding the activation energies listed in Table 2. Also shown are the coupling model predictions for the JG relaxation times, from the experimental values of τ_α and β_{KWW}, with $t_c = 2$ ps.

Table 2. Activation Energies (kJ/mol) at $P = 0.1$ MPa

	α-process[a]	β-process	γ-process
PCHMA	396 ± 7	90.5 ± 2.6	51.3 ± 0.6
50/50 blend	507 ± 7		46.0 ± 0.8

[a] At $\tau_\alpha = 10$ s.

In Figure 6 are representative lower temperature spectra showing another, more prominent, secondary relaxation. Designated the γ-relaxation (but unrelated to the τ_α scaling exponent referred to above and defined in eq 4), this process involves conformational transitions of the cyclohexyl ring (chair-to-chair flipping motion).[38,39] The γ-relaxation times for the neat and blended PCHMA are shown in Figure 5; the former have a steeper slope, corresponding to $\sim10\%$ larger activation energy E_γ (Table 2). The preexponential factor $\log(\tau_0/\text{s}) = -14.3 \pm 0.1$ and -13.2 ± 0.2 for neat PCHMA and the blend. At frequencies beyond the γ-relaxation in Figure 6, the dielectric loss is flat. This almost frequency-invariant response is known as the nearly constant loss (NCL).[40]
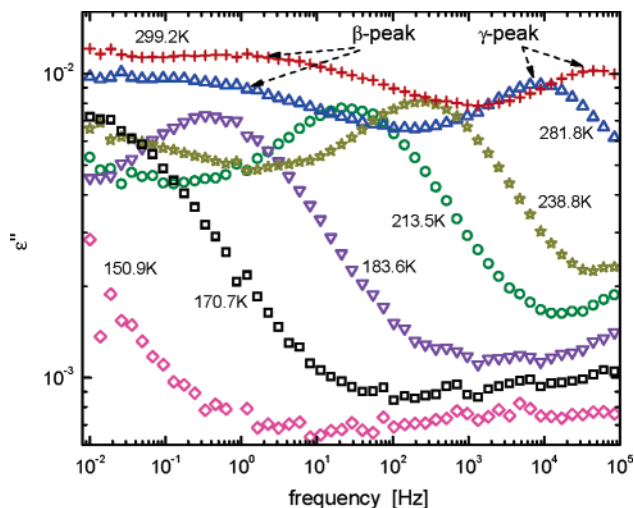
Figure 6. Dielectric loss for neat PCHMA at low temperatures, showing the γ-peak. At the two higher temperatures the β-peak is moving in from the low-frequency side. At temperatures < 184 K the NCL is evident in the spectra at frequencies beyond the γ-peak.

3.3. Elevated Pressure Results. The dielectric spectra were measured as a function of pressure at various temperatures. Because of interference from dc conductivity (especially a problem at higher temperatures), only the α-relaxation could be accurately characterized at high P. As shown previously for neat PCHMA and its blend with PaMS,[34] the breadth of the local segmental relaxation dispersion is constant at fixed τ_α; this is illustrated in Figure 7.

The pressure dependences of τ_α for neat PCHMA and its blend are displayed semilogarithmically in Figure 8. The data are linear, suggesting a simple parametrization using[41]

$$\Delta V^{\#} = RT \left. \frac{\partial \ln \tau_\alpha}{\partial P} \right|_T \tag{2}$$

in which $\Delta V^{\#}$ is the activation volume. In accord with many other studies,[42−45] we find $\Delta V^{\#}$ decreases with increasing T, from 159 to 204 mL/mol for neat PCHMA and 175 to 265 mL/ mol for the blend, over a comparable temperature range of ca. 45 K.

To interpret the high-pressure data, these pressure dependences are converted to volume dependences, requiring the equation of state (EOS). This was calculated for the liquid state from PVT measurements, fit to the Tait EOS[35]

$$V(T,P) = (a_0 + a_1T + a_2T^2)\{1 - C\ln[1 + P/(b_0e^{-b_1T})]\} \tag{3}$$

with T in °C and a_0, a_1, a_2, C, b_0, and b_1 being T- and P-independent constants. The values of these parameters from the two neat polymers and the 50% blend samples are listed in Table 3. Figure 9 shows the data for the blend measured from 10 to 100 MPa over the temperature range from 303 to 423 K along with the fit to eq 3.

As shown in Figure 10, and in accord with previous results for relaxation times[9,46] and viscosities[47] of various glass-forming materials, τ_α for PCHMA, both neat and blended with PaMS, conforms to the scaling law

$$\tau_\alpha = \mathscr{F}(TV^{\gamma}) \tag{4}$$

where $\mathscr{F}$ is some function. Thus, τ_α, obtained at atmospheric pressure vs temperature and at various fixed temperatures vs pressure, collapse onto a single curve for $\gamma = 2.5 \pm 0.15$ and
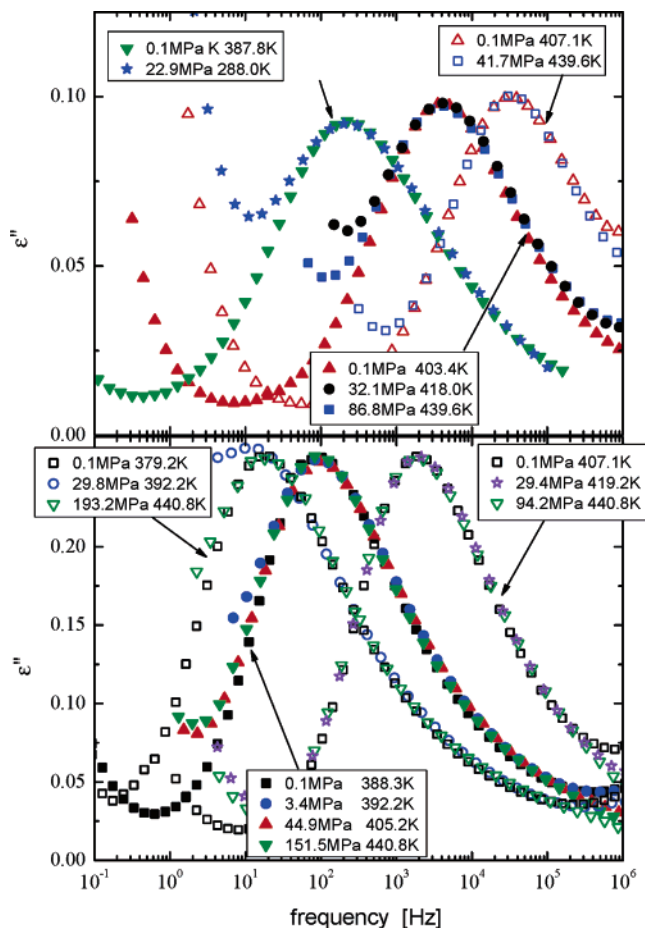

Figure 7. Local segmental relaxation peaks for various T and P such that τ_α is essentially constant: (bottom) neat PCHMA (top) PCHMA/ PaMS 50/50 blend. Spectra were shifted slightly to superpose the peak maxima. The rise in the dielectric loss toward low frequency, especially prominent in the blend spectra, is due to dc conductivity.
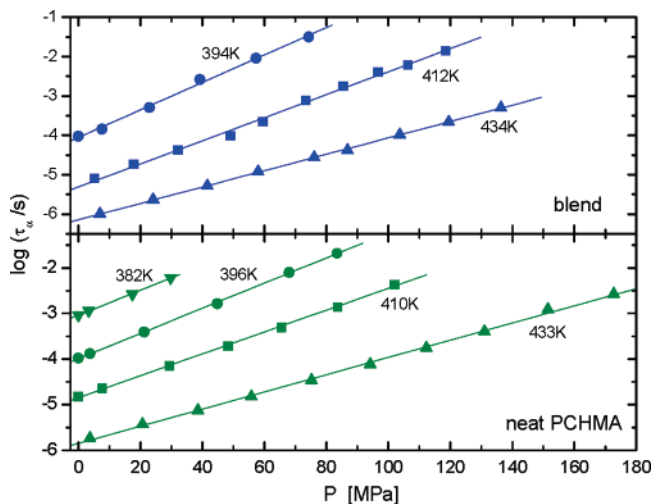

Figure 8. Variation of τ_α for neat (lower) and blended (upper) PCHMA with hydrostatic pressure. The slopes of the indicated linear fits yield the activation volumes (eq 2).

3.7 ± 0.15 respectively for neat PCHMA and its blend. (Note that for blends the application of eq 4 requires that only one component contribute to the response, since each polymer can have different T or P dependences; this condition is fulfilled for PCHMA mixed with the weakly polar PaMS. An underlying assumption is that the V is eq 4, which is obtained on the blend, is a relevant measure of the specific volume of the PCHMA
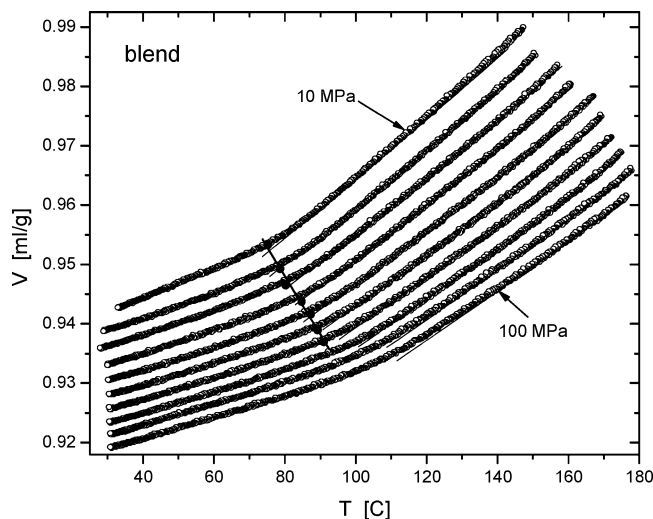
Figure 9. Specific volume vs temperature for the PCHMA/PaMS blend at pressures from 10 to 100 MPa (10 MPa increments). The solid circles are the pressure-dependent T_g determined from the intersection of the extrapolated liquid and glassy data. The thin solid lines are fits to the liquid-state data, and the thick solid line is the fit to the pressure-dependent T_g.
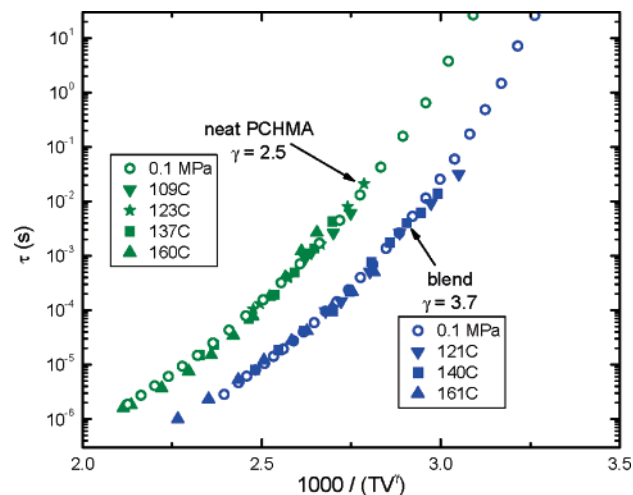

Figure 10. Scaled plots of the local segmental relaxation times (ambient pressure isobar and isotherms as indicated).

component; this point is considered below.) The error in the scaling exponent primarily reflects uncertainty in the temperature of the high-pressure measurements. Larger γ for the blend means that volume exerts a stronger influence than in neat PCHMA.

4. Discussion

4.1. Fragility of Local Segmental Relaxation. A common measure of the temperature dependence of the dynamics of glass-forming materials is the fragility, $m = (\mathrm{d}\log\tau_\alpha)/(\mathrm{d}T_g/T)|_{T_g}$.[48] In Figure 11 τ_α are plotted in this T_g-normalized Arrhenius form, from which the values of m listed in Table 1 were obtained. Addition of PaMS significantly increases m of PCHMA (although since this quantity represents the T_g-normalized temperature dependence of the most probable relaxation times, any effect on fragility from the change in the
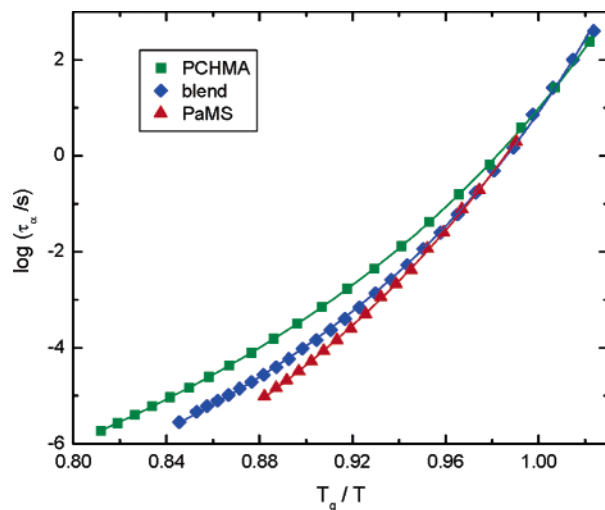

Figure 11. T_g-normalized temperature dependence of local segmental relaxation times for PCHMA, PaMS, and their blend.

breadth of the dielectric loss peak, as seen in Figure 2, is ignored). Although the PaMS has a lower T_g, evidently PaMS segments impose constraints on local motion of the PCHMA segments in the blend, giving rise to the longer τ_α at low temperatures (Figure 1) and the increase in m. This interpretation follows from the general idea that the magnitude and T dependence of τ_α in supercooled liquids and polymers are governed primarily by intermolecular cooperativity.[49] Interestingly, while PaMS has a lower T_g than neat PCHMA, it has a larger fragility, while the apparent activation energy at T_g for the blend is equal with the experimental error to that for neat PaMS.

Generally, it has been found that longer chain length results in greater fragility,[50–54] although the effect is weak or absent in very flexible chain polymers.[55,56] Recent results on the related material, poly(methyl methacrylate) (PMMA), revealed an increasing m with molecular weight;[54,57] however, this increase is evident only for very small M_w, the effect saturating when the concentration of chain ends becomes small. Fitting to eq 1 the combined dielectric data from refs 32 and 33 for a high molecular weight PCHMA ($M_w = 65$ kg/mol), we obtain $m = 53 \pm 6$. This roughly equals the fragility of the sample studied herein (with $M_w = 3.4$ kg/mol), for which $m = 58.5 \pm 0.5$. We expect that at smaller chain length a significant dependence of m on M_w could be observed, as seen in PMMA.[57]

4.2. Thermodynamic Scaling of τ_a. The local segmental relaxation times for PCHMA conform to the thermodynamic scaling (eq 4), both neat and in the 50% blend with PaMS. The former is consistent with results on more than 50 different glass-forming materials, including molecular and ionic liquids as well as polymers.[9,47] The fact that the α-peaks superpose when measured under conditions of T and P such that τ_α is constant (Figure 7) means that the breadth of the α-dispersion depends only on the relaxation time.[34,58,59] Together with the results in Figure 10, this means that a single material constant, γ, defines both the segmental relaxation time and the shape of the segmental relaxation function.

The motivation for this scaling comes from approximating the intermolecular potential as a generalized inverse power-law

Table 3. Tait EOS (Eq 3)

	a_0 (mL/g)	a_1 (mL/g C)	a_2 (mL/g C^2)	C	b_0 (MPa)	b_1 (C)
PCHMA	0.9310 ± 0.0002	$(2.50 \pm 0.02) \times 10^{-4}$	$(1.99 \pm 0.02) \times 10^{-6}$	0.0611	233 ± 1	$(8.66 \pm 0.04) \times 10^{-3}$
50/50 blend	0.9210 ± 0.0005	$(4.50 \pm 0.09) \times 10^{-4}$	$(3.42 \pm 0.40) \times 10^{-7}$	0.0894	228 ± 2	$(2.95 \pm 0.01) \times 10^{-3}$
PaMS	0.9375 ± 0.0003	$(4.50 \pm 0.06) \times 10^{-4}$	$(5.78 \pm 0.28) \times 10^{-7}$	0.0894	271 ± 2	$(4.04 \pm .06) \times 10^{-3}$

repulsive potential.[47,60] However, more recently we have shown that eq 4 follows from any model expressing the relaxation times in terms of the configurational entropy, and thus γ can be related to the Grüneisen parameter.[60−62] For blends the thermodynamic scaling has been demonstrated previously for only two cases: PVME with polystyrene[63] and with poly(2-chlorostyene).[64] A problem with application of eq 4 to blends is that the actual component volume is unknown since the EOS only specifies the total volume. For polymers having similar α_T and κ_T the relative volume of either component should not depend strongly on thermodynamic conditions, so that V for the blend volume can be used in determining γ of a component. Nevertheless, to corroborate the use of the blend specific volume, we can deduce the scaling exponent for the blend by an alternative procedure and compare the result to the value obtained by superpositioning the τ_α, which of course is specific to the PCMHA component. We calculate γ from the equation[65]

$$\alpha_\tau = -(\gamma T_g)^{-1} \qquad (5)$$

where α_τ is the thermal expansion coefficient for constant value of τ_α. Since T_g corresponds to constant τ_α,[9] α_τ can be obtained from the change with pressure in the specific volume at the glass transition temperature, V_g; that is, $\alpha_\tau = \mathrm{d} \ln(V_g)/\mathrm{d}T_g$. These V_g are taken as the intersection of the extrapolated liquid and glassy state isobars (see Figure 9), from which we obtain at 10 MPa and $T_g = 348.4$ K, $\alpha_\tau = -7.54 \times 10^{-4}$ K^{-1} for the blend. Equation 5 then gives $\gamma = 3.8$, in satisfactory agreement with the value determined from superposition of the τ_α, $\gamma = 3.7 \pm 0.15$. Since γ for the blend is equivalent to the scaling exponent for the PCHMA component, an implication is that the dynamics of both components are described by roughly the same γ.

4.3. Relative Contribution of Energy and Volume to τ_a. While the magnitude of the scaling exponent reflects the relative contribution of volume to the dynamics, a more common measure of volume and temperature effects is the ratio of the isochoric activation energy, E_V ($\equiv R(\mathrm{d} \ln \tau)/\mathrm{d}T^{-1}|_V$) to the isobaric activation enthalpy, H_P ($\equiv R(\mathrm{d} \ln \tau)/\mathrm{d}T^{-1}|_P$).[9,66] This ratio is related to the scaling exponent according to[46]

$$E_V/H_P = (1 + \gamma T \alpha_P)^{-1} \qquad (6)$$

where α_P is the isobaric thermal expansion coefficient, determined from *PVT* data. While γ is a constant, E_V/H_P changes with T and P.[67] This is shown in Figure 12 for neat PCHMA and its blend at $P = 0.1$ MPa. These results reveal how volume effects become more dominant as temperature is reduced. This is at odds with classic free volume interpretations of the glass transition,[36] based on the assumption that unoccupied space governs the dynamics. The idea that large thermal energy fluctuations are required to circumvent large potential barriers arising under the congested conditions prevailing at low temperature is not supported by the results in Figure 11. At higher temperature, for which the T dependence becomes weaker approaching Arrhenius behavior (Figure 3), the unoccupied volume increases, yet τ_α becomes less dependent on temperature; that is, the more free volume that is available, the less effect volume has on the dynamics.

Although the relative contribution of V and T varies with temperature (Figure 12) for any given T, volume effects remain stronger in the blend than in neat PCHMA, as expected from the larger scaling exponent for the blend ($\gamma = 3.7$ vs 2.5). We also find that when compared at the same temperature (or equal value of τ_α), the activation volume for the blend is larger than $\Delta V^\#$ for neat PCHMA; this enhanced sensitivity to pressure
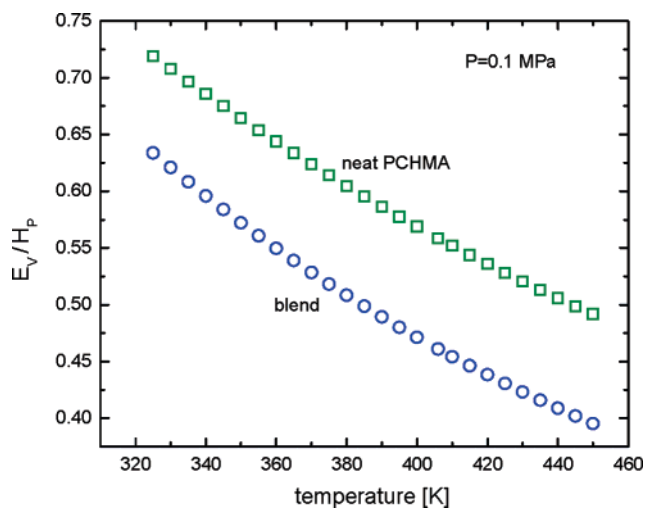

Figure 12. Ratio of the isochoric and isobaric activation enthalpies as a function of temperature, showing the decreasing influence of V with increasing T. The asymptotic values of E_V/H_P are zero and unity, corresponding to V-dominated and T-dominated dynamics, respectively.

reflects the greater influence of volume in the former. The magnitude of $\Delta V^\#$ per se varies from about 1 to 1.4 times the molar volume of the PCHMA repeat unit.

4.4. Secondary Relaxations. The identity of the secondary β-process in PCHMA is controversial. Absent from light scattering[68] and mechanical spectra,[32] the β-relaxation appears as a weak peak in the dielectric loss (Figure 4). Heijboer[39] ascribed this process to partial rotation of the carboxyl group. On the other hand, Murthy and Shahin[33] suggested that one or two repeat units of the PCHMA chain participate in the β-relaxation; that is, the process involves intermolecular degrees of freedom and thus is a Johari−Goldstein relaxation. This term refers to the precursor of structural relaxation believed to be present, if not always perceived, in all glass-forming liquids and polymers.[69] The most probable Johari−Goldstein relaxation time, τ_{JG}, is predicted to follow the "unconstrained" (or primitive) relaxation time, τ_0, of the coupling model[8,69]

$$\tau_{JG} \sim \tau_0 = t_c^{1-\beta_{KWW}} \tau_\alpha^{\beta_{KWW}} \qquad (7)$$

where $t_c = 2$ ps. The Johari−Goldstein relaxation times are calculated from eq 7 using the values for the Kohlrausch exponent determined from fitting the α-peak for neat PCHMA to the KWW function:[28] for temperatures from 349 to 369 K, $\beta_{KWW} = 0.44 \pm 0.01$. As seen in Figure 5, there is no correspondence between the calculated τ_{JG} and the experimentally measured τ_β. Since eq 7 has been shown to be valid for many materials,[69,70] the implication is that the β-relaxation in PCHMA is not a JG process. This calculation assumes that the peak breadth is reflective of the local segmental dynamics only. In acrylate polymers with bulky alkyl groups, the possibility exists for a second α-relaxation involving the pendant group.[71] This would broaden the dispersion, confounding determination of β_{KWW}, and thus obviate an analysis based on eq 7.

In light of eq 7, if the β-process in PCHMA were a JG relaxation, blending would be expected to alter τ_β, since the properties of the α-process, such as τ_α and the fragility (Figure 11), change with blending. However, τ_β is sensibly invariant to the presence of the PaMS (Figure 5), consistent with its origin as a side-group motion, involving only intramolecular degrees of freedom, rather than a JG motion of the entire PCHMA repeat unit.

The γ-relaxation for neat PCHMA has an activation energy, $E_\gamma = 51.3$ kJ/mol, and has been identified as a chair-to-chair conformational change of the alkyl ring.[39] However, similar to the result for E_β, the activation energy determined herein is substantially larger than reported for a much higher molecular weight PCHMA, for which $E_\gamma = 45$ kJ/mol.[33] These are in the general range for the chair-to-chair change in cyclohexanes.[72] We observe only a small effect from blending on the γ-process, which is tempting to ascribe to a small volume being swept out during the ring motion. Similarly, it has been found that the dynamics of pendant cyclohexyl groups on various acrylate polymers are only weakly dependent on the chemical nature of the backbone or matrix.[73−75] Note that, consistent with this idea, the breadth of the γ-peak is relatively narrow.

The dielectric loss of PCHMA at the lowest temperatures (Figure 6) reveals an NCL. This spectral feature is common in ionic conductors and has been seen previously in dielectric relaxation measurements on polyisoprene[76] and polybutadiene[77] as well as in light scattering measurements on polyisobutylene[78] and polymethamethacrylate.[79] In most polymers the NCL is obscured by secondary relaxations, so that its observation is limited to very low temperatures. But since the magnitude of the NCL decreases exponentially with decreasing temperature,[76−78,80] high-resolution instruments are then required to detect the NCL. In Figure 6 the NCL for PCHMA is approximately constant with frequency. Any increase could be ascribed to the presence of other high-frequency processes. A vanishingly weak δ-process has been reported at very high frequencies in PCHMA.[32,39]

4.5. Anomalous Blend Dynamics. Calorimetry, *PVT*, and dielectric relaxation measurements (Figure 1 and Table 1) all show that the local segmental dynamics of PCHMA are slowed by the addition of PaMS. The particular temperatures for the glass transitions vary with the experimental technique and are in accord with the expectation that higher rates yield higher values of T_g: *PVT* at 0.5 K/min < DSC at 10 K/min < dielectric $\tau_\alpha(T_g) = 10$ s (the corresponding rate for the latter substantially exceeds 10 K/min).[9]

This slowing down of the blend dynamics is an anomaly because the PaMS has a lower T_g and accordingly shorter τ_α. The most common equation for the T_g of a blend is due to Fox[81]

$$T_g(\phi_A) = \left(\frac{\phi_A}{T_{g,A}} + \frac{1 - \phi_A}{T_{g,B}}\right)^{-1} \quad (8)$$

in which $T_{g,A}$ and $T_{g,B}$ are the respective glass transition temperatures of components A and B and ϕ_A is the volume fraction ($\sim$ weight fraction herein) of A. Obviously, the Fox equation is incapable of reproducing the maxima in the concentration dependence of T_g for the PCHMA blend (Figure 1). Other relations for $T_g(\phi_A)$ have been proposed,[82−85] including the nonlinear equation of Brekner[86,87]

$$T_g(\phi_A) = T_{g,A} + (T_{g,A} - T_{g,B})[(1 + K_1)(1 - \phi_A) - (K_1 + K_2)(1 - \phi_A)^2 + K_2(1 - \phi_A)^3] \quad (9)$$

where K_1 and K_2 are constants. As shown in Figure 1, eq 9 describes the qualitative features of the data, albeit requiring the use of two adjustable parameters, $K_1 = -3.4 \pm 0.7$ and $K_2 = -3.4 \pm 1$.

An approach to account for the dynamics of polymer blends is the LM model,[25] in which the relaxation properties of the components are governed by the local composition within each subvolume. The model builds on the idea that the local composition of a component is enhanced by chain connectiv-ity,[88−91] with the subvolume having a length scale determined by the Kuhn step length, l_K, of the polymer chain. The effective local concentration within this subvolume, ϕ_{eff} (which exceeds the average concentration, ϕ_A), is given by[25]

$$\phi_{eff} = \phi_{self} + \phi_A(1 - \phi_{self}) \quad (10)$$

in which ϕ_{self} is the "self-concentration" of A within a subvolume V_{self}. The operative assumption is that the blend dynamics are just the cumulative result of a distribution of "local" glass transition temperatures, $T_g(\phi_A)$, for each subvolume.[92] Adapting eq 8 to the local subvolumes gives[25]

$$T_g(\phi_A) = \left(\frac{\phi_{eff}}{T_{g,A}} + \frac{1 - \phi_{eff}}{T_{g,B}}\right)^{-1} \quad (11)$$

Note that unless ϕ_{eff} is the same for the two components, two T_g's are expected, with eq 11 giving the value for the component with that particular ϕ_{eff}. A significant difference between ϕ_{self} for the two components requires a correction to eq 11, as pointed out by Lipson and Milner,[93] in order that the composition averaged over all subvolumes equals the bulk ϕ_A.

The appeal of the LM model is that ϕ_{self} can be calculated from the chain properties, so that in principle the blend dynamics are predicted without adjustable parameters. In practice, ϕ_{self} is often varied empirically to yield agreement with experimental data.[64,94−96] Since the Fox equation is incapable of describing the calorimetric glass transition behavior in Figure 1, we make the analogous modification of eq 9, replacing ϕ_A with ϕ_{eff}

$$T_g(\phi_A) = T_{g,A} + (T_{g,A} - T_{g,B})[(1 + K_1)(1 - \phi_{eff}) - (K_1 + K_2)(1 - \phi_{eff})^2 + K_2(1 - \phi_{eff})^3] \quad (12)$$

in order to analyze the dielectric τ_α for the blend. Using the values of K_1 and K_2 from fitting the calorimetric T_g, we obtain the result is shown in Figure 1, with $\phi_{eff} = 0.60$ yielding the best fit of τ_α for $\phi_A = 0.5$. Equation 10 then gives $\phi_{self} = 0.20$. This self-concentration can be compared to the value estimated from the properties of the PCHMA chain[25]

$$\phi_{self} = \frac{C_\infty m_0 V}{n N_A V_{self}} \quad (13)$$

in which the repeat unit molecular weight $m_0 = 167$ g/mol, the number of backbone bonds per repeat unit $n = 2$, $V(T_g) (=V_g) = 0.9629$ mL/g, and N_A is Avogadro's number. The size of the subvolume, V_{self}, is on the order of $l_K{}^3$.[25] Using literature values for PCHMA,[97] $l_K = 17.7$ Å and the characteristic ratio $C_\infty = 11.6$, from eq 13 we calculate $\phi_{self} = 0.27 \pm 0.01$. This is in acceptable agreement with the experimental value of 0.20, considering the accuracy of eq 9 and the fact that V_{self} is only approximated. It should also be noted that the LM assumes that this subvolume defining the concentration fluctuations is tem-perature-invariant, whereas the cooperative length scale increases with decreasing temperature.[88,91]

There remains to explain the anomaly that the blend τ_α and T_g are not intermediate between the neat component values. This peculiarity was seen previously in several mixtures in which the components had nearly equal T_g: polychloroprene with epoxidized polyisoprene,[98] polybutadiene with poly(chlorinated biphenyl),[99−101] polystyrene with poly(chlorinated biphenyl),[102] polymethylphenylsiloxane with 1,1′-bis(p-methoxyphenyl)cy-clohexane,[103] and polyepichlorohydrin with poly(vinyl methyl ether).[104,105] However, except for the latter blend, these materials all exhibited the opposite effect—the dynamics became *faster*

upon addition of a *higher* T_g component. Two explanations have been proposed for such behavior. The first considers the change in volume due to blending, i.e., the excess volume. If this is negative, it will increase congestion and contribute to a slowing down of the dynamics. From the *PVT* data we obtain the specific volumes of the PCHMA and PaMS at the ambient pressure glass transition; these V_g are listed in Table 1. Assuming additivity of the volumes, the specific volume calculated for the blend is 0.966 mL/g, while experimentally $V_g = 0.958$ mL/g for the blend. Thus, the excess volume is negative, and this volume contraction could account for the anomalous increase of τ_α in the blend.

A second explanation for anomalous blend dynamics is based on the coupling model,[99,100] which considers the contribution to the observed relaxation times from intermolecular constraints. Since these constraints can change upon blending, their effect on the dynamics may not be directly inferable from properties of the neat components. Thus, while the T_g of neat PaMS is lower than that of neat PCHMA, this may be due in part to intermolecular constraints which are irrelevant to the blend. Specifically, if the local friction factor *increases* upon addition of the PaMS, the relaxation of the PCHMA may slow down (as observed). Friction factor in this context refers to constraints on local motion other than those arising from intermolecular cooperativity (steric constraints or specific interactions). To assess the magnitude of this friction factor, we remove the effect of intermolecular cooperativity by using the coupling model to calculate the relaxation time in the absence of coupling; this is the τ_0 in eq 7. The argument is that while at a given temperature τ_α of neat PaMS is less than τ_α of neat PCHMA, τ_0 of the former could be larger than τ_0 for PCHMA. If so, this would contribute to a slowing down of the PCHMA dynamics in the blend.

Near T_g the Kohlrausch exponent for PaMS is 0.31 ± 0.01, whereas for PCHMA $\beta_{KWW} \sim 0.44$. Since β_{KWW} is smaller for PaMS, by inspection of eq 7 we see that $\tau_0^{PCHMA}/\tau_0^{PaMS} < \tau_\alpha^{PCHMA}/\tau_\alpha^{PaMS}$; that is, removal of intermolecular coupling (by consideration of the τ_0 rather than τ_α) would lead to even greater *speeding up* of the PCHMA dynamics. Thus, the prediction from the coupling model is opposite to the experimental observation. Consideration of the relative friction factors for the neat components only emphasizes the anomaly observed herein; its origin cannot be accounted for by changes in intermolecular cooperativity as described by the coupling model.

Finally, we note that the increase in τ_α and T_g upon blending could arise from chemical reaction between the components, whereby the relaxing entity in the blend becomes chemically coupled to neighboring segments. Specific interactions can also make the mixing less random.[106] The thermodynamic miscibility of styrene polymers with acrylates, as reflected in the value of the LCST, is greater for the α-substituted polymer (such as PaMS used herein) than for other polystyrenes. This implies a more negative mixing enthalpy and stronger interaction. Chang and Woo[29] reported changes in the vibrational spectrum due to blending PCHMA with PaMS, indicating interaction of the carbonyl group of the acrylate with the phenyl ring of PaMS. However, the vibrational perturbations are small, suggesting the interactions are weak. Moreover, if the dynamics of the β-relaxation involve rotation of the carbonyl group,[39] the fact that this process is little affected by blending is inconsistent with significant chemical interaction (Figure 5). Further work is required to judge whether any specific interactions between the PCHMA and PaMS are sufficient to contribute to the qualitative anomaly in the blend dynamics seen herein.

5. Summary

From the EOS and high-pressure dielectric measurements of τ_α, we show that the segmental relaxation times for both neat PCHMA and its blend with PaMS superpose as a function of TV^γ, with γ increasing from 2.5 to 3.7 upon blending. The latter value is independently determined from the change in the glass transition temperature with pressure in combination with eq 5; thus, the specific volume of the blend, as opposed to some ill-defined component volume, is the relevant scaling quantity, at least for this material. The larger value of γ for the blend indicates the stronger influence of volume on the dynamics, as similarly reflected in a larger activation volume. In accord with previous results on various glass-forming liquids and polymers, the parameter γ uniquely defines both the α-relaxation time and its distribution.

The dielectric relaxation measurements reveal an interesting anomaly in this blend—the segmental relaxation times of the PCHMA become longer, even though the added PaMS has a lower T_g and shorter τ_α than neat PCHMA. This result is at least qualitatively consistent with the negative excess (mixing) volume. Using the Brekner equation[86] for the composition dependence of T_g, we deduce a Lodge—McLeish[25] self-concentration for the PCHMA, $\phi_{self} = 0.20$, in accord with the value estimated from the Kuhn step length of the PCHMA chain.

Unlike the local segmental dynamics, the two secondary relaxations in the dielectric spectra are unaffected by blending, consistent with their identification as intramolecular modes of motion (i.e., not the Johari—Goldstein process). At the lowest temperatures, a nearly constant loss becomes apparent at high frequencies.

References and Notes

(1) Ngai, K. L.; Roland, C. M. *Polymer* **2002**, *43*, 567.
(2) Kisliuk, A.; Mathers, R. T.; Sokolov, A. P. *J. Polym. Sci., Polym. Phys.* **2000**, *38*, 2785.
(3) Thurau, C. T.; Ediger, M. D. *J. Chem. Phys.* **2003**, *118*, 1996.
(4) Cicerone, M. T.; Blackburn, F. R.; Ediger, M. D. *Macromolecules* **1995**, *28*, 8224.
(5) Hooker, J. C.; Torkelson, J. M. *Macromolecules* **1995**, *28*, 7683.
(6) Garwe, F.; Schonhals, A.; Lockwenz, H.; Beiner, M.; Schroter, K.; Donth, E. *Macromolecules* **1996**, *29*, 247.
(7) Arbe, A.; Colmenero, J.; Frick, B.; Monkenbusch, M.; Richter, D. *Macromolecules* **1998**, *31*, 4926.
(8) León, C.; Ngai, K. L.; Roland, C. M. *J. Chem. Phys.* **1999**, *110*, 11585.
(9) Roland, C. M.; Hensel-Bielowka, S.; Paluch, M.; Casalini, R. *Rep. Prog. Phys.* **2005**, *68*, 1405.
(10) Paluch, M.; Casalini, R.; Roland, C. M. *Phys. Rev. B* **2002**, *66*, 092202.
(11) Shears, M. S.; Williams, G. *J. Chem. Soc., Faraday Trans. 2* **1973**, *69*, 608.
(12) Wetton, R. E.; MacKnight, W. J.; Fried, J. R.; Karasz, F. E. *Macromolecules* **1978**, *11*, 158.
(13) Roland, C. M. *Macromolecules* **1987**, *20*, 2557.
(14) Lau, S.-F.; Pahtak, J.; Wundelich, B. *Macromolecules* **1982**, *15*, 1278.
(15) Cifra, P.; Karasz, F. E.; MacKnight, W. J. *Macromolecules* **1988**, *21*, 446.
(16) Roland, C. M. *Rubber Chem. Technol.* **1989**, *62*, 456.
(17) Chung, G. C.; Kornfield, J. A.; Smith, S. D. *Macromolecules* **1994**, *27*, 964.
(18) Miller, J. B.; McGrath, K. J.; Roland, C. M.; Trask, C. A.; Garroway, A. N. *Macromolecules* **1990**, *23*, 4543.
(19) Ngai, K. L.; Roland, C. M. *Macromolecules* **1995**, *28*, 4033.
(20) Roland, C. M.; Ngai, K. L. *Macromolecules* **1991**, *24*, 2261.
(21) Zetsche, A.; Fischer, E. W. *Acta Polym.* **1994**, *45*, 168.
(22) Katana, G.; Fischer, E. W.; Hack, Th.; Abetz, V.; Kremer, F. *Macromolecules* **1995**, *28*, 2714.
(23) Kamath, S.; Colby, R. H.; Kumar, S. K.; Karatasos, K.; Floudas, G.; Fytas, G.; Roovers, J. E. L. *J. Chem. Phys.* **1999**, *111*, 6121.

(24) Kamath, S.; Colby, R. H.; Kumar, S. K. *Phys. Rev. E* **2003**, *67*, 010801.

(25) Lodge, T.; McLeish, T. C. B. *Macromolecules* **2000**, *33*, 5278.

(26) Haley, J. C.; Lodge, T. P.; He, Y.; Ediger, M. D.; von Meerwall, E. D.; Mijovic, J. *Macromolecules* **2003**, *36*, 6142.

(27) Cangialosi, D.; Alegria, A.; Colmenero, J. *Macromolecules* **2006**, *39*, 7149.

(28) Ngai, K. L.; Roland, C. M. *Rubber Chem. Technol.* **2004**, *77*, 579.

(29) Chang, L. L.; Woo, E. M. *Polym. J.* **2001**, *33*, 13.

(30) Ishida, Y.; Yamafuji, K. *Kolloid Z.* **1961**, *177*, 97.

(31) Heijboer, J. *Makromol. Chem.* **1960**, *35A*, 86.

(32) Ribes-Greus, A.; Gomez-Ribelles, J.; Diaz-Calleja, R. *Polymer* **1985**, *26*, 1849.

(33) Murthy, S. S. N.; Shahin, Md. *Eur. Polym. J.* **2006**, *42*, 715.

(34) Roland, C. M.; Casalini, R. *J. Non-Cryst. Solids*, in press (cond-mat/0701258).

(35) Zoller, P.; Walsh, D. J. *Standard Pressure-Volume-Temperature Data for Polymers*; Technomic: Lancaster, PA, 1995.

(36) Ferry, J. D. *Viscoelastic Properties of Polymers*, 3rd ed.; Wiley: New York, 1980.

(37) Hedvig, P. *Dielectric Spectroscopy of Polymers*; Adam Hilger: Bristol, 1977.

(38) Kotlik, P.; Heidingsfeld, V.; Zelinger, J. *J. J. Polym. Sci., Polym. Chem.* **1975**, *13*, 1417.

(39) Heijboer, J. *Ann. N.Y. Acad. Sci.* **1976**, *279*, 104.

(40) Jonscher, A. K. *Dielectric Relaxation in Solids*; Chelsea Dielectric Press: London, 1983.

(41) Floudas, G. In *Broadband Dielectric Spectroscopy*; Kremer, F., Schonhals, A., Eds.; Springer-Verlag: Berlin, 2003; Chapter 8.

(42) O'Reilly, J. M. *J. Polym. Sci.* **1970**, *57*, 429.

(43) Roland, C. M.; Casalini, R.; Santangelo, P. G.; Sekula, M.; Ziolo, J.; Paluch, M. *Macromolecules* **2003**, *36*, 4954.

(44) Casalini, R.; Roland, C. M. *J. Chem. Phys.* **2003**, *119*, 4052.

(45) Papadopoulos, P.; Peristeraki, D.; Floudas, G.; Koutalas, G.; Hadjichristidis, N. *Macromolecules* **2004**, *37*, 8116.

(46) Casalini, R.; Roland, C. M. *Phys. Rev. E* **2004**, *69*, 062501.

(47) Roland, C. M.; Bair, S.; Casalini, R. *J. Chem. Phys.* **2006**, *125*, 124508.

(48) Angell, C. A. *J. Non-Cryst. Solids* **1991**, *13*, 131−133.

(49) Ngai, K. L.; Roland, C. M. *Macromolecules* **1993**, *26*, 6824.

(50) Santangelo, P. G.; Roland, C. M. *Macromolecules* **1998**, *31*, 4581.

(51) Roland, C. M.; Casalini, R. *J. Chem. Phys.* **2003**, *119*, 1838.

(52) Leon, C.; Ngai, K. L.; Roland, C. M. *J. Chem. Phys.* **1999**, *110*, 11585.

(53) Mattsson, J.; Bergman, R.; Jacobsson, P.; Börjesson, L. *Phys. Rev. Lett.* **2003**, *90*, 075702.

(54) Ding, Y.; Novikov, V. N.; Sokolov, A. P.; Cailliaux, A.; Dalle-Ferrier, C.; Alba-Simionesco, C.; Frick, B. *Macromolecules* **2004**, *37*, 9264.

(55) Roland, C. M.; Ngai, K. L. *Macromolecules* **1996**, *29*, 5747.

(56) Paluch, M.; Roland, C. M.; Pawlus, S. *J. Chem. Phys.* **2002**, *116*, 10932.

(57) Casalini, R.; Roland, C. M.; Capaccioli, S. *J. Chem. Phys.*, submitted.

(58) Ngai, K. L.; Casalini, R.; Capaccioli, S.; Paluch, M.; Roland, C. M. *J. Phys. Chem. B* **2005**, *109*, 17356.

(59) Ngai, K. L.; Casalini, R.; Capaccioli, S.; Paluch, M.; Roland, C. M. In *Advances in Chemical Physics;* Kalmykov, Y. P., Coffey, W. T., Rice, S. A., Eds.; Wiley: New York, 2006; Vol. 133B, Chapter 10.

(60) Roland, C. M.; Feldman, J. L.; Casalini, R. *J. Non-Cryst. Solids* **2006**, *352*, 4895.

(61) Casalini, R.; Mohanty, U.; Roland, C. M. *J. Chem. Phys.* **2006**, *125*, 014505.

(62) Roland, C. M.; Casalini, R. *J. Phys.: Condens. Matter*, in press (cond-mat/0610428).

(63) Roland, C. M.; Casalini, R. *Macromolecules* **2005**, *38*, 8729.

(64) Roland, C. M.; McGrath, K. J.; Casalini, R. *Macromolecules* **2006**, *39*, 3581.

(65) Roland, C. M.; Casalini, R. *J. Chem. Phys.* **2005**, *122*, 134505.

(66) Williams, G. In *Dielectric Spectroscopy of Polymeric Materials*; Runt, J. P., Fitzgerald, J. J., Eds.; American Chemical Society: Washington, DC, 1997; Chapter 1.

(67) Roland, C. M.; McGrath, K. J.; Casalini, R. *J. Non-Cryst. Solids* **2006**, *352*, 4910.

(68) Fytas, G. *Macromolecules* **1989**, *22*, 211.

(69) Ngai, K. L.; Paluch, M. *J. Chem. Phys.* **2004**, *120*, 857.

(70) Ngai, K. L. *J. Chem. Phys.* **1998**, *109*, 6982.

(71) Beiner, M.; Huth, H. *Nat. Mater.* **2003**, *2*, 595. Ngai, K. L.; Beiner, M. *Macromolecules* **2004**, *37*, 8123.

(72) Davies, M.; Swain, J. *Faraday Soc. Trans.* **1971**, *67*, 1637.

(73) Ngai, K. L.; Gopalakrishnan, T. R.; Beiner, M. *Polymer* **2006**, *47*, 7222.

(74) Domínguez-Espinosa, G.; Sanchis, M. J.; Díaz-Calleja, R.; Pagueguy, C.; Gargallo, L.; Radic, D. *Polymer* **2005**, *46*, 11351.

(75) Heijboer, J. In *Molecular Basis of Transitions and Relaxations*; Midland Molecular Monographs; Meier, D. J., Ed.; Gordon and Breach: London, 1984.

(76) Roland, C. M.; Schroeder, M. J.; Fontanella, J. J.; Ngai, K. L. *Macromolecules* **2004**, *37*, 2630.

(77) Schroeder, M. J.; Ngai, K. L.; Roland, C. M. *J. Polym. Sci., Polym. Phys. Ed.* **2007**, *45*, 342.

(78) Sokolov, A. P.; Kisluik, A.; Novikov, V. N.; Ngai, K. L. *Phys. Rev. B* **2001**, *63*, 172204.

(79) Caliskan, G.; Kisluik, A.; Sokolov, A. P.; Novikov, V. N. *J. Chem. Phys.* **2001**, *114*, 10189.

(80) Kudlik, A.; Benkhof, S.; Blochowicz, T.; Tschirwitz, C.; Rössler, E. *J. Mol. Struct.* **1999**, *479*, 210.

(81) Fox, T. G. *Bull. Am. Phys. Soc.* **1956**, *1*, 123.

(82) Couchman, P. R.; Karasz, F. E. *Macromolecules* **1978**, *11*, 177.

(83) Gordon, M.; Taylor, J. S. *J. Appl. Chem.* **1962**, *2*, 493.

(84) Di Marzio, E. A. *Polymer* **1990**, *31*, 2294.

(85) Kwei, T. K.; Pearce, E. M.; Pennacchia, J. R.; Charton, M. *Macromolecules* **1987**, *20*, 1174.

(86) Brekner, M. J.; Schneider, H. A.; Cantow, H. J. *Polymer* **1988**, *29*, 78.

(87) Leroy, E.; Alegría, A.; Colmenero, J. *Macromolecules* **2002**, *35*, 5587.

(88) Kant, R.; Kumar, S. K.; Colby, R. H. *Macromolecules* **2003**, *36*, 10087.

(89) Eric, L.; Alegria, A.; Colmenero, J. *Macromolecules* **2002**, *35*, 5587.

(90) Cangialosi, D.; Schwartz, G. A.; Alegria, A.; Colmenero, J. *J. Chem. Phys.* **2005**, *123*, 144908.

(91) Krygier, E.; Lin, G.; Mendes, J.; Mukandela, G.; Azar, D.; Jones, A. A.; Pathak, J. A.; Colby, R. H.; Kumar, S. K.; Floudas, G.; Krishnamoorti, R.; Faust, R. *Macromolecules* **2005**, *38*, 7721.

(92) Zetsche, A.; Fischer, H. W. *Acta Polym.* **1994**, *45*, 168.

(93) Lipson, J. E. G.; Milner, S. T. *J. Polym. Sci., Polym. Phys. Ed.* **2006**, *44*, 3528.

(94) Haley, J. C.; Lodge, T. P.; He, Y.; Ediger, M. D.; von Meerwall, E. D.; Mijovic, J. *Macromolecules* **2003**, *36*, 6142.

(95) He, Y.; Lutz, T. R.; Ediger, M. D. *J. Chem. Phys.* **2003**, *119*, 9956.

(96) Lutz, T. R.; He, Y.; Ediger, M. D.; Cao, H.; Lin, G.; Jones, A. A. *Macromolecules* **2003**, *36*, 1724.

(97) Wu, S. *Polym. Eng. Sci.* **1992**, *32*, 823.

(98) Roland, C. M.; Santangelo, P. G.; Baram, Z.; Runt, J. *Macromolecules* **1994**, *27*, 5382.

(99) Rizos, A.; Ngai, K. L. *Phys. Rev. B* **1992**, *46*, 8126.

(100) Santangelo, P. G.; Roland, C. M.; Ngai, K. L. *Macromolecules* **1994**, *27*, 3859.

(101) Roland, C. M. *Macromolecules* **1995**, *28*, 3463.

(102) Casalini, R.; Santangelo, P. G.; Roland, C. M. *J. Phys. Chem. B* **2002**, *106*, 11492.

(103) Roland, C. M.; Santangelo, P. G.; Ngai, K. L.; Meier, G. *Macromolecules* **1993**, *26*, 6164.

(104) Alegria, A.; Telleria, I.; Colmenero, J. *J. Non-Cryst. Solids* **1994**, *172*, 961.

(105) McGrath, K. J.; Roland, C. M. *Rubber Chem. Technol.* **1994**, *67*, 629.

(106) Plans, J.; MacKnight, W. J.; Karasz, F. E. *Macromolecules* **1984**, *17*, 810.